Indian Journal of Pure & Applied Physics
Vol. 56, November 2018, pp. 859-868

Fabrication of low cost and versatile internal field pulsed nuclear magnetic resonance spectrometer to study the magnetic materials

B M Siddesh[a], M Manjunatha[b], Ramakrishna Damle[b] & K P Ramesh[a]*

[a]Department of Physics, Indian Institute of Science, Bengaluru 560 012, India
[b]Department of Physics, Bangalore University, Bengaluru 560 056, India

Received 9 October 2017; accepted 15 May 2018

We have built a low cost and versatile pulsed internal field nuclear magnetic resonance (IFNMR) spectrometer and used it to study ferromagnetic materials. Initially optimization of the instrument has been tested with nuclear quadrupole resonance (NQR) active nuclei. Ferromagnetic materials like bulk iron, bulk cobalt and carbon coated cobalt nanopowder have been used as the testing materials for our spectrometer. Preliminary results obtained from the present spectrometer have been compared with the earlier reports and are in good agreement. The specifications and performance standard of the instrument match quite well with standard instruments elsewhere in the world which is testified with the observation of NMR echo signals in the above mentioned materials confirming the quality of the spectrometer. Additionally NMR signals from the grain boundaries are observed in Co@C nanomaterials which prove the sensitivity of the spectrometer.

Keywords: Ferromagnetic nanomaterials, IFNMR spectrometer, RF enhancement, ^{57}Fe, ^{59}Co, Co@C

1 Introduction

Nuclear magnetic resonance (NMR) is a useful technique to study various kinds of materials, since it provides information regarding the physical and chemical properties of the nuclei under study. NMR active nuclei in paramagnetic and the diamagnetic materials are studied in the presence of external magnetic field. However, NMR in ferromagnetic materials do not require an external magnetic field because of the presence of inbuilt magnetic field (hyperfine field), hence it is also called as internal field NMR (IFNMR). NMR studies in magnetic materials provide wide range of information including local structure, presence of foreign bodies in the system (non-magnetic material)[1,2], metal to insulator phase purity and many other exotic properties. In recent years ferromagnetic nanomaterials are gaining interest because of their feasible application in various fields such as magnetic toners, xerography, contrast agents, drug delivery, magnetic hyperthermia and other uses[3-6]. Furthermore, spintronic materials exhibit exotic magnetic properties with different local structures which can be better explored using local probe like IFNMR. Further, most of the physical and chemical properties are particle size dependent. For example bulk iron is ferromagnetic when its size is in μm, whereas it exhibits superparamagnetism when the size gets reduced to nanometre[7] (<10 nm). The transition from ferro to superparamagnetic can be best observed using the IFNMR technique, since local hyperfine field plays an important role during this transition. In spite of these wide range of applications, IFNMR spectrometers to study these ferromagnetic nanomaterials are very few in the country to the best of our knowledge, as commercial NMR spectrometers for this purpose are not available. Considering all the above mentioned facts, we have built a low cost versatile pulsed IFNMR spectrometer and the details of which are provided in this communication. In the first part of this communication we have discussed briefly the origin of magnetism in the ferromagnetic materials and their NMR resonance, while in the second part we have described the fabrication of the IFNMR spectrometer and its performance with the standard samples.

2 Origin of Magnetism in the Ferromagnetic Materials

2.1 Internal field of ferromagnetic materials

The internal field (hyperfine field) in the ferromagnetic materials arises from various contributions. The origin of hyperfine field in the ferromagnetic materials is well discussed by Marshall

*Corresponding author
(E-mail: kpramesh@iisc.ac.in, keralapuraramesh@gmail.com)

et al.[8], Freeman *et al.*[9], Stearns *et al.*[10] and Wurmehl *et al.*[2]. According to them, the internal field is an effective sum of the following terms:

$$H_{\text{int}} = H_{Loc} + H_{hf} \quad \ldots (1)$$

(where, H_{Loc} is the local magnetic field at the nucleus, H_{hf} is the effective magnetic field due to the hyperfine field). The local magnetic field H_{loc} at the nucleus is further given by:

$$H_{Loc} = H_E + H_D + H_{Lorentz} + H' \quad \ldots (2)$$

(where, H_E is external magnetic field , H_D is demagnetizing field, $H_{Lorentz} = \frac{4}{3}\pi m$ is the Lorentz field, H' *is* residual Lorentz field due to the non-cubic symmetry). External field term (H_E) is zero in the case of ferromagnetic materials since no external magnetic field is applied. Demagnetizing field (H_D) depends on the shape of the specimen, which exists only in the single domain but cancels out in the multi domain particles. Effect of demagnetizing field can be estimated by observing the shift in the central frequency in the presence of an external magnetic field. Lorentz field $(\frac{4}{3}\pi M)$ has its origin due to the electron magnetic moments acting on the nuclear magnetic moments. The value of M (saturation magnetization) is different for various ferromagnetic materials (Co-1710 gauss, Fe-1446 gauss and Ni-510 gauss). H' is considered to be zero for the cubic symmetry.

The H_{hf} term involves the contributions from the three major terms:

$$H_{hf} = H_{dip} + H_{orb} + H_{FC} \quad \ldots (3)$$

where, H_{dip} is the dipolar field due to interaction between the nuclear magnetic moments and the d shell electrons outside the nucleus in the same atom. H_{orb} arises due to the presence of non-quenched orbital moments of valence electrons. H_{FC} is the field due to Fermi contact term which arises due to the polarization of core electrons (H_{core}), conduction electrons (H_{cond}) and transferred hyperfine field (H_{trans}):

$$H_{FC} = H_{core} + H_{cond} + H_{trans} \quad \ldots (4)$$

The electrons from the 1s, 2s, 3s (core electrons) involve in exchange interaction with the magnetic moment of on-site 3d electrons resulting in the core polarization. H_{cond} is due to the spin polarization of the conduction s electrons with the on-site magnetic moment of the nucleus itself. H_{trans} is transferred hyperfine field which occurs due to the hybridization of polarized d-orbital with s electrons. A sum of all these contributions yield an estimated internal field for bulk iron (~33 T), cobalt (~21 T) and for nickel (~6.5 T).

2.2 Resonance in the ferromagnetic materials

In case of NMR active nuclei in non-magnetic materials, the role of external magnetic field is to lift the degeneracy of Zeeman energy levels with a redistribution of their population in energy levels[11] (low spin state and the high spin states). The numbers of spins in the lower energy are slightly more than the higher energy level. It is possible to excite these spins from lower to higher energy level with suitable radiation with ΔE satisfying the condition:

$$\Delta E = \frac{\gamma H_0}{2\pi} \quad \ldots (5)$$

(where, γ is the gyromagnetic ratio of the nuclei, h is the Planck's constant, H_o is the applied magnetic field). This energy difference can be varied by varying the magnetic field and generally it falls in the range of radiofrequency (~10^6 MHz). The spins in the lower energy levels will absorb this radiation and makes the transition from low energy (m=+1/2) state to high energy state (m= –1/2). The transition of the nuclear spins (population difference) is governed by the Boltzmann equation[12,13]:

$$\frac{m = -1/2}{m = +1/2} = e^{-\frac{\gamma H_0}{KT}} \quad \ldots (6)$$

(where, γ is the gyromagnetic ratio of the nuclei, H_o is the applied magnetic field, K is the Boltzmann constant , T is the absolute temperature).

As mentioned in the introduction in the case of ferromagnetic material the degeneracy energy levels are lifted by the internal field at the site of nuclei. The energy difference between these two levels is almost fixed because of internal field and its distribution. The suitable radio frequency can cause transition from lower to the upper energy level. Since the internal field is inhomogeneous in ferromagnetic materials, the resonance is spread over a range, but the NMR signal can still be easily observed with increased

signal to noise ratio. This can be attributed to RF enhancement (increased S/N) which occurs only in the ferromagnetic materials in contrast to the para and diamagnetic materials.

2.2.1 RF enhancement

RF enhancement arises because of the inherent property of the ferromagnetic materials due to the existence of domains and domain walls[14]. Domains are formed in these materials to reduce their magneto static energy. Domains are further separated by the domain walls. The applied RF field induces oscillations in the electronic moments of the ferromagnetic material[2]. These oscillations lead to changes in the hyperfine field due to their coupling via the hyperfine interaction, resulting in an RF component of the hyperfine field. Now the resultant RF field is a sum of applied RF and induced RF at the nucleus, hence one can expect a higher enhancement of signal to noise ratio. The extent of RF enhancement is different in domain and domain wall correspondingly the intensities of the NMR spin echo signal is also different and occur at different frequencies. The spatial variation of magnetic moments in the domain walls are different leading to a greater enhancement compared to the domains, as the domains are pinned. Hence it is expected that NMR signal intensity in the domain wall is enhanced compared to domains. Due to the RF enhancement in ferromagnetic materials one can apply very low power (0.1 –5 watt) to observe the IFNMR signals.

Among the different magnetic nuclei in ferromagnetic materials, ^{57}Fe and ^{59}Co are widely studied because of their wide range of applications.

^{57}Fe (2.2% abundance) has I=1/2, resulting in two possible energy levels (–1/2 and +1/2) due to the internal field. The transition from +1/2 to –1/2 (Δm=±1) is according to the selection rule. The resonance frequency can be calculated using the Larmor equation[2,11-13]:

$$f = \frac{\gamma H_0}{2\pi} \quad \ldots (7)$$

(where, γ is the gyromagnetic ratio (for iron 1.38×10^6Hz/T) and H_0 is the internal field). The calculated RF frequency for the bulk iron is typically ~45.5 MHz at RT.

^{59}Co (100% abundance) has I=7/2 therefore it has eight energy levels. However these energy levels are equally spaced for a cubic symmetry leading to a single resonance signal[2]. The internal field of cobalt is ~21 T. The resonance frequency is calculated using the Eq. (7) and it is found to be ~213 MHz. However in cobalt there is a slight difference between the internal field corresponding to Hexagonal Closed Packing (*hcp)* and Face Centered Cube (*fcc)* phases which leads to difference in the NMR frequency.

3 Fabrication of the Spectrometer

IFNMR spectrometers can be classified into two main types depending on the type of RF used one is Continuous Wave spectrometer (CW) and the other is pulsed spectrometers. CW NMR spectrometers are obsolete now a day due to the following reasons: continuous wave spectrometer requires different active components to cover the wide range of frequencies, which limits their application as FM resonance is spread over a wide range of frequencies (~20-500 MHz). Further it cannot be inter-phased with the modern averaging techniques and modulation techniques which are necessary for the signal detection. To overcome these limitations we have chosen to build a pulsed IFNMR spectrometer. Commercial and indigenous components are integrated in the present spectrometer depending on their specification and availability.

3.1 IFNMR spectrometer and its parts

The block diagram of the homemade spectrometer is shown in the Fig. 1 with various modules. IFNMR instrument is mainly divided into three main divisions, i.e., transmitter, probe and receiver part. The transmitter part includes pulse blaster, signal generator, power splitter, double balanced mixer, power amplifier. The purpose of the transmitter is to transmit the suitable energy (ΔE) in the form RF pulse to the probe. The Parallel LC probe which contains a sample induces the voltage due to the transition of nuclear spins from lower to upper lever which leads to change in the magnetic flux of the inductor coil. Receiver part contains preamplifier, phase sensitive detector (PSD), RC low pass filter and the digital storage oscilloscope (DSO). The receiver part receives the induced voltage and can be visualised as echo in the DSO. The working of each module is discussed below.

3.1.1 Transmitter

3.1.1.1 Spin core pulse blaster

The pulses are used for the three different purposes in our spectrometer (1) to produce the mixed output of applied radiofrequency, (2) blanking input for the

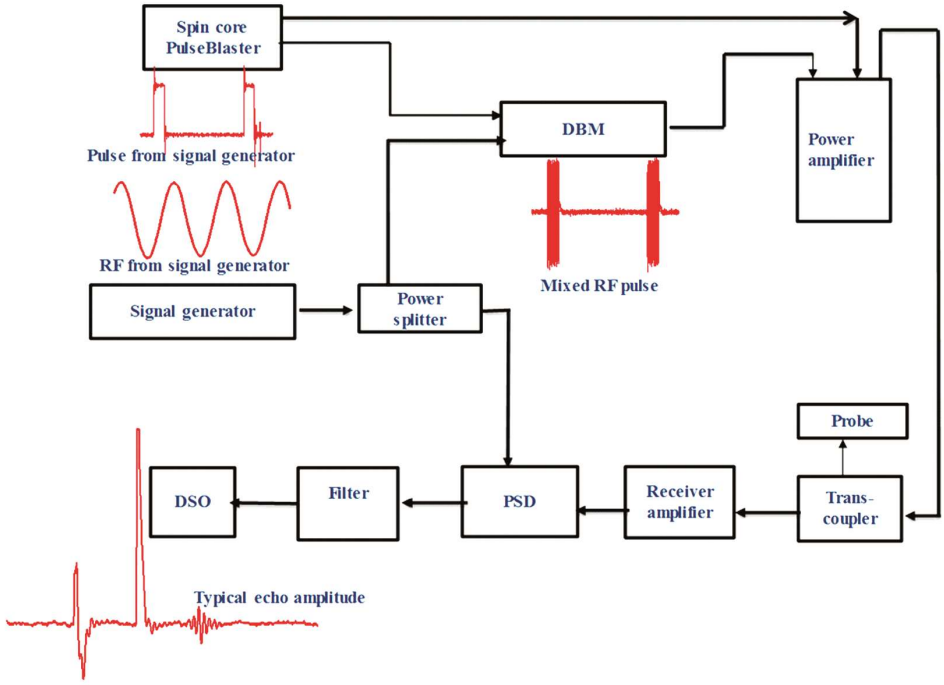

Fig. 1 — Block diagram of homemade pulsed IFNMR spectrometer.

power amplifier, (3) external triggering for the oscilloscope. For this purpose a multichannel pulse generator is essential. These requirements are met using a Spin Core Pulse Blaster model (PB24-100-4k) which can produce 24 independent pulses and the shortest duration of the pulse is 50 ns with a pulse resolution of 10 ns. This is procured from M/S Spin Core technologies, USA. The desired pulses are produced using a spin core pulse interpreter program using software which is available in the website[15]. The typical pulse produced using the pulse generator is given in the block diagram (Fig. 1).

3.1.1.2 Signal generator

The required resonance Larmor frequency is produced using Agilent signal generator (model: 8605 A), with a variable voltage output in the frequency from 1-1000 MHz. The output voltage used for our experiment is less than 20 mV due to the RF enhancement. Typical RF wave produced from our signal generator is given in the block diagram (Fig. 1).

3.1.1.3 Power splitter

The radio frequency output from the signal generator is connected to the power splitter. We have used the mini circuits (*ZFC-2-1+*) power splitter, covering the range 5 to 500 MHz. One of the output of the power splitter is connected to the input of the double balance mixer and the other is used as reference for phase sensitive detection (PSD).

3.1.1.4 Double balanced mixer (DBM)

Double balanced mixer helps in mixing the continuous RF wave with the pulses. We have used a three stage mixing (HP make (model: 10514 A)) DBM, which can operate from 0.2 to 500 MHz) with rise and fall times less than 1ns. The mixed RF output is amplified before giving it to the power amplifier. Typical mixed RF output obtained from the DBM is shown in the block diagram (Fig. 1).

3.1.1.5 Power amplifier

The transition of the spins from the lower to the higher level happens with certain high power (typically 0.1- 5 W for ferromagnetic materials). The power produced at the DBM is not enough to observe the resonance hence, a power amplifier (PA) is essential. We have used AMT power amplifier (model: 3205) which works efficiently in the range of 10-235 MHz with a gain of 60 dB.

The output from the DBM is connected to the power amplifier. The output of power amplifier is connected to the input of transcoupler. The required power levels can be controlled by varying the input voltage from the signal generator.

3.2 Transcoupler (Transmitter–receiver switch)

The transcoupler is a device which is used to switch the transmitter and the receiver section

alternately. It consists of three ports namely transmitter, probe and the receiver port. The output of

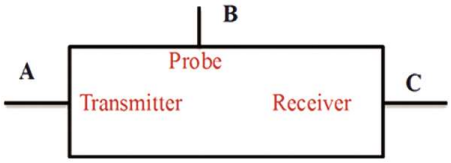

Fig. 2 — Block diagram of transcoupler used in the present spectrometer.

the power amplifier is connected to the transmitter port, the probe is connected to the probe port and the pre amplifier is connected to the receiver port. The block diagram of the typical transcoupler is shown in Fig. 2. When the RF pulse is given to the probe via coupler the receiver part is disconnected which protects the receiver. When the transmitter output is turned off, the receiver conducts and induced voltage produced at the probe coil due to the change in the magnetic flux from the sample. This induced voltage reaches to the pre-amplifier. The transcoupler used in the present work was procured from NMR service, Germany.

3.3 Probe

A tuned circuit with impendence matching is essential (50 Ω) to couple the RF power to the sample and induced voltage from sample to the receiver. Since, in the entire spectrometer all the devices have 50 Ω matching impendence the entire circuit uses a 50 Ω cable for all the connection (Huber-Suhnermake). We have used a parallel resonance probe circuit with a matching capacitor/inductor. Point A shown in Fig. 3(a) and Fig. 3(b) is connected to the probe port (B) of the transcoupler. The matching capacitor/ inductor coils are used to match the impendence of the circuit (50 Ω) at a given frequency. This matching of the impendence is very essential for the lossless transmission. The formulae used to calculate the inductor and capacitor values are as follows:

a) $f = \dfrac{1}{2\pi\sqrt{LC}}$

b) $X_C = \dfrac{1}{2\pi fc}$

c) $X_L = 2\pi fL$

(where, f is the resonance frequency, L is the inductance of inductor used, C is the capacitance of capacitor used, X_c is the capacitive reactance and X_L is the inductive reactance). We have used variable trimmer capacitors in the range 1-20 pf for the

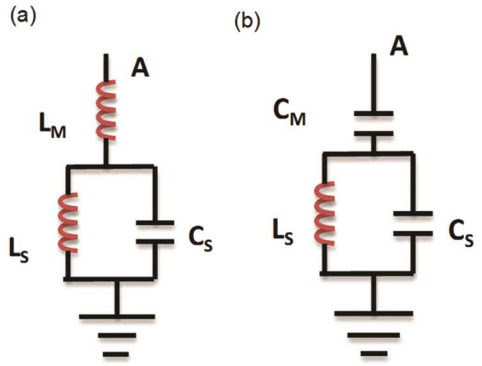

Fig. 3 — Block diagram of probe coil (a) inductor matched probe coil and (b) capacitor matched probe coil.

frequency range used in the present study. The sample is placed in the sample coil L_s which is hand wound depending on the frequency. The samples are filled in quartz/glass tube and sealed before placing it in the sample coil.

3.4 Receiver section

3.4.1 Receiver amplifier

The induced voltage produced at the probe coil is very small (1≤μV), so to amplify the received signals we have used a preamplifier. The input of the receiver amplifier which has a gain of 65 dB with a recovery time less than 1 μs (as specified by the manufacturer) (Narda Mite Q AU-1467) is connected to the receiver port of the transcoupler. The induced voltage is amplified at this stage and connected to the phase sensitive detector.

3.4.2 Phase sensitive detector (PSD)

To match the phase of the induced voltage produced at the resonance frequency, with the input radiofrequency, a DBM can be used as the PSD. The output of the pre amplifier/receiver is connected to the RF port of the phase sensitive detector. The reference signal obtained from the power splitter is connected to LO port of DBM. The output from the PSD is obtained from the IF port and passed through a low pass filter.

3.4.3 Low pass filter

Output from the PSD contains NMR signals which are in phase with input radiofrequency. But along with a signal there will be always associated noise at various frequencies. To eliminate these high frequencies we have used a RC low pass filter. The output signal from the IF port of the PSD is connected to input of the filter. The output of the filter is fed to the digital storage oscilloscope for further processing of the signal.

3.4.4 Digital oscilloscopescope (DSO)

The signal obtained during the resonance (induced voltage) is visualized in the DSO. We have used Tektronics make (model 2012) DSO. 128 on line signal averaging on the DSO is done before transferring the signal to a flash drive or to the computer. Further higher number of averages can be done with an inter phase to the computer. Typical IFNMR spin echo signal is shown in the block diagram (Fig.1).

The entire receiver section can also be replaced and inter-phased with the National Instruments (NI USB-5133, 2-ch, 100MS/s, digitizer W/32 mb/ch memory) module or any other digital receiver system for digitization and signal averaging with Lab View user software.

4 Practical Considerations for the Operation of the Spectrometer

4.1 Pulsesequences

The ferromagnetic signals are very broad due to the spread of hyperfine field unlike the paramagnetic and diamagnetic counterparts; hence the selection of pulse sequence plays a very crucial role in observing the resonance signals. We have used a spin echo sequence ($\pi/2-\tau-\pi$) and solid echo ($\pi/2-\tau-\pi/2$) for our experiments. In both the cases, the $\pi/2$ pulse is assigned for the pulse where maximum echo amplitude is observed, τ is the delay between the two pulses.

4.2 Tuning of the probe coil

As mentioned earlier, power is coupled to the sample kept in an induction coil which should be tuned to have 50 Ω impendence and to zero phase difference simultaneously (inductive reactance is equal to capacitive reactance, which is necessary condition for the LC resonance). The tuning of LC probe manually for a wide range of frequency ranging from 10-300 MHz is quite cumbersome. We circumvented this situation by a simplified approach of using two different LC probe circuits, one covering from 40-100 MHz range and the other from 100-300 MHz, which will facilitate us to study major ferromagnetic materials like iron, iron oxides (ferrites) and the cobalt (as these frequencies range from 40-280 MHz). The advantage of our tuning method is that the quality factor $\left(\frac{f_0}{2\Delta f}\right)$of the resonance circuit (which measures the sharpness of the LC parallel resonance) is maintained constant over a range of frequencies for a particular sample using a compact hand held impedance analyzer (Rig Expert make, 1-600 MHz).

Further, in ferromagnetic materials, NMR echo signals are spread over a large frequency range, hence it is very much necessary to tune the probe accordingly. In our experiments the probe coil is tuned for every 0.5 MHz for cobalt and 0.05 MHz for iron specifically which can be different for other samples.

4.3 Data collection and plotting

Since the ferromagnetic signals are very broad, depending on the width of the signal spin echo amplitude is noted either from the computer or manually from the oscilloscope and is plotted as a function of frequency.

4.4 Low temperature experiments

Measurements at 77 K are done using a specially designed homemade co-axial extended line probe. The versatility of this probe is that it can be used for all the frequencies with a slight modification (change of coil or capacitors). Low temperature probe is shown in the Fig. 4.

Fig. 4 — Home-made low temperature probe.

5 Optimization and Specifications of the Fabricated IFNMR Spectrometer

5.1 Optimization

The IFNMR spectrometer is first tested for nuclear quadrupole resonance (NQR) signals from standard samples at room temperature like para-dichlorobenzene (PDB) at 34.24 MHz, potassium chlorate ($KClO_3$) at 29.3 MHz and copper (II) oxide (Cu_2O) at 26.02 MHz. The ^{35}Cl and ^{63}Cu NQR signals in these samples were observed with a very good signal to noise ratio. The pulse widths used for these samples were in the range of 10 to 15 μs. After this stage, the search for IFNMR signals of ^{59}Co and ^{57}Fe is taken up. While looking for these signals, one should keep in mind the RF enhancement and accordingly adjust the signal generator output.

5.2 Specifications achieved of our fabricated IFNMR spectrometer

(i) The recovery time (dead time) of the entire instrument should be less than 10 μs because the typical ferromagnetic signals are very broad hence the echo signal can be observed only for a short duration of the delay between the pulses. We have also achieved recovery time less than 5 μs, which is capable of observing the broad signals (for example NMR signals from cobalt nanomaterials).

(ii) The excitation pulse width is quite small (less than 1 μs) as the signal of ferromagnetic sample usually is spread over a wide range. Our spectrometer is capable of producing the RF pulses of 50 ns duration.

(iii) To cover the various IFNMR in ferromagnetic materials containing Fe, Co and Ni nuclei the spectrometer should be capable of operating over a wide range of frequency (typically from 10 to 250 MHz). Our spectrometer at present can operate between 10-235 MHz, additionally it can be upgraded to 400 MHz using high frequency amplifier (235-400 MHz).

(iv) Miniature probe is required so that less volume of sample can be used. We have used a probe with a sample coil of 2-6 mm diameter with only 2-4 numbers of turns. Further the complete list of the specifications is given in the Table 1.

6 Materials and Characterization

For the present study we have obtained the bulk iron (average particle size 3μ, purity 97 %) and carbon coated cobalt nanopowder (Co@C) from the M/S Sigma Aldrich, and the bulk cobalt (average particle size 2 μ, purity 99.5%), from M/s Alfa Aesar. These particles are characterized by the 'Panalytical' powder XRD. Figure 5(a) shows the powder XRD of the bulk cobalt, Co@C and 5(b) shows bulk iron. From the XRD measurements it is clear that bulk cobalt exhibits peaks corresponding to *fcc* [(111), (200), (220)] and *hcp*[(100), (101)] phases. On the other hand Co@C has only *fcc* phase [(111), (200), (220)]. The presence of *fcc* and *hcp*, absence of *hcp*

Table 1 — Specifications of present low cost versatile IF pulsed NMR spectrometer

Spectrometer Type	Pulsed
Range of frequency	1– 400 MHz
Recovery time	$\leq$ 5 μs
Types of materials	Ferromagnetic, ferrimagnetic materials
Active nuclei	^{57}Fe, ^{59}Co, ^{61}Ni, ^{55}Mn
Pulse sequences	Spin echo, "two equal pulses" sequences
RF power amplifier gain	60 dB
Receiver amplifier gain	65 dB
Operating temperature	77- 300 K
Data collection type	Digital/ manual

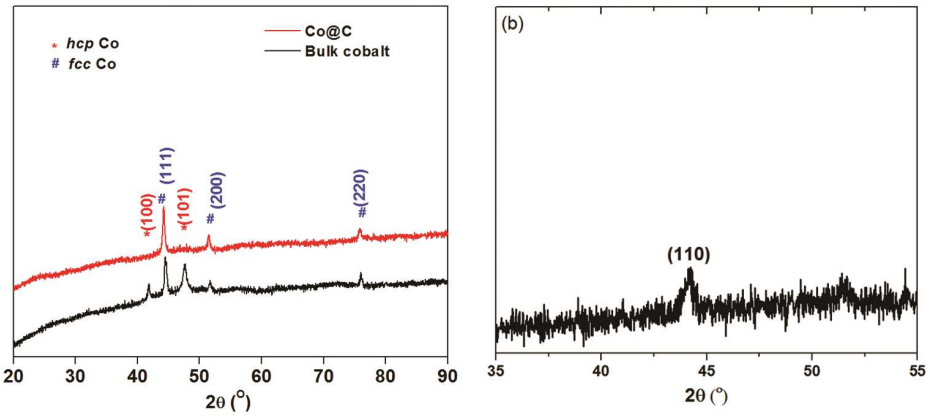

Fig. 5 — XRD plots for (a) bulk cobalt powder and Co@C sample (b) bulk iron powder.

phase in the Co@C has been confirmed using our IFNMR spectrometer (discussed in the following section). Bulk iron has only one peak corresponding to (110), which confirms the existence of *bcc* iron.

7 Results and Discussion

7.1 Cobalt (^{59}Co)

XRD studies by Hull *et al.*[16] has shown that the cobalt exists in two forms viz., *hcp* and *fcc*. Our XRD results also confirm the presence of these phases in the bulk cobalt powder. ^{59}Co IFNMR studies were reported in the early 60's by Gossard *et al.*[14,17]. Later Kawakami *et al.*[18] reported the *hcp* phase of the cobalt through IFNMR. Later Bromer *et al.*[19] and Toth *et al.*[20] independently reported IFNMR studies and concluded that cobalt exists in two phases (*fcc* and *hcp*) along with stacking *s1, s2, s3* and *s4*. Recently Bastow *et al.*[21] reviewed cobalt studies. Andreev *et al.*[22] have given a new insight to the phases of cobalt and concluded both the phases coexist in the same sample. Keeping these studies in background we have taken up IFNMR studies in Cobalt. We have used spin echo pulse sequence with 0.5 μs as π/2 pulse and τ of 25 μs.

Figures 6(a) and 6(b) show the ^{59}Co NMR spectra observed using the present spectrometer for bulk cobalt at 300 K and 77 K, respectively. Our observations at 300 K are in good agreement with the earlier reports. Main peaks around 213 MHz corresponds to domain walls of *fcc* phase while the peaks around 215.5, 217 and 218.4 MHz at 300 K corresponds to the phase with stacking faults *s1, s2* and *s3*, respectively. Two other peaks observed around 220 and 223 MHz correspond to domain walls of *hcp* and stacking fault *s4*, respectively. Further the frequencies corresponding to *fcc* and *s1, s2, s3* were shifted to higher value of 219.5, 221.5 and 222.5 MHz, respectively, at 77 K. Similarly the frequencies corresponding to *hcp* domain wall and stacking fault *s4* shift to higher value of 223 MHz and 228 MHz at 77 K. Shift in the frequencies at 77 K in both the cases is due to the increase in the spontaneous magnetization of cobalt.

The shift in the resonance frequency for *hcp* cobalt from *fcc* is well documented[14,17-22]. According to those reports, the *hcp* phase of cobalt experiences slight higher the internal field (21.8 T) compared to *fcc* phase of cobalt (21.13 T). From Eq. (7) it is clear that resonance frequency depends linearly on the internal field, hence one can expect the resonance frequency of *hcp* phase of cobalt (220 MHz at RT) occur at slightly higher value compared to *fcc* phase (213 MHz). The presence of stacking faults is due to the alternate stack formation during the formation of *fcc* and *hcp* phases.

7.2 Iron (^{57}Fe)

Internal field studies of Iron was first reported by Hanna *et al.*[23], in the year 1960 using Mössbauer studies and it was found to be 33 T. Robert *et al.*[24] and Budnick *et al.*[25]independently reported the IFNMR studies of iron. Recently Bastow *et al.*[21] reviewed the iron IFNMR studies and reported the resonance frequency of iron is ~45.5 MHz at room temperature (300 K).With this background we have looked for iron IFNMR signal in bulk iron. We have used spin echo pulse sequence with π/2 pulse 1 μs and τ of 50 μs.

Figures 7(a) and 7(b) show the ^{57}Fe NMR spectra for bulk iron at 300 K and 77 K respectively. Our measurement on the iron matches very well with the earlier reports[21,24,25]. At 77 K there is a shift in the NMR frequency which is attributed to the increase in the spontaneous magnetization.

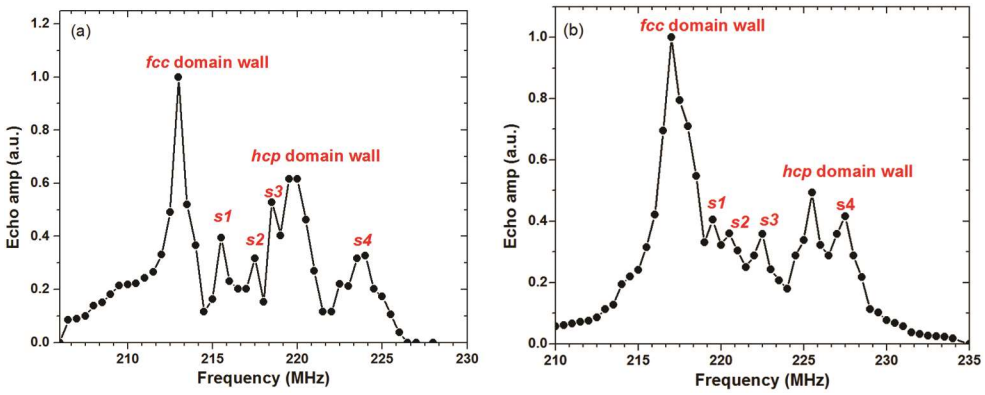

Fig. 6 — A plot of echo amplitude as a function of frequency obtained from present spectrometer for bulk cobalt (^{59}Co NMR) (a) 300 K and (b) 77 K

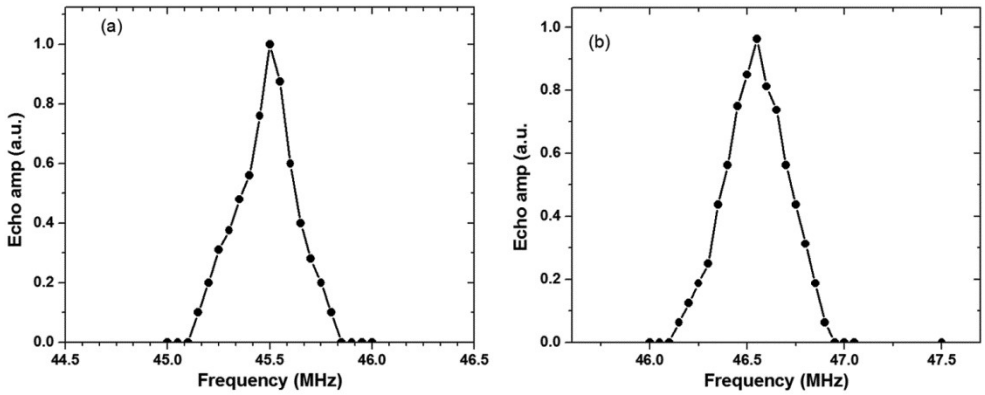

Fig. 7 — A plot of echo amplitude as a function of frequency obtained from present spectrometer for bulk iron (^{57}Fe NMR) (a) 300 K and (b) 77 K

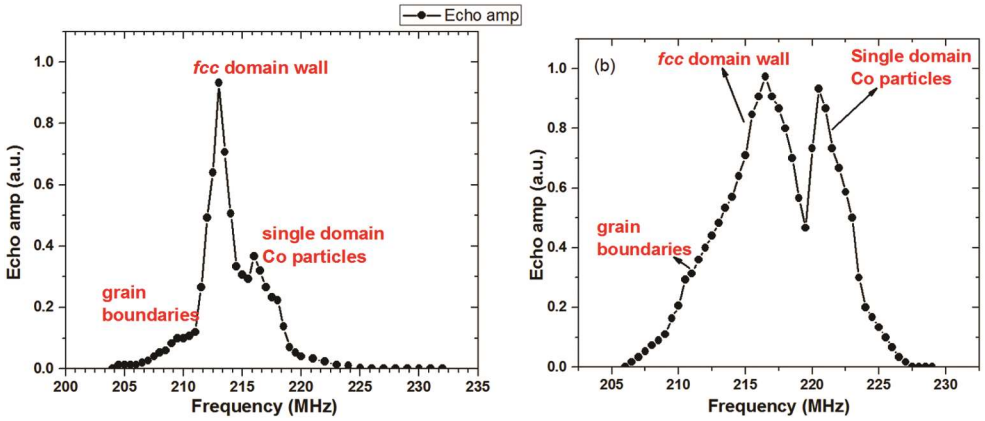

Fig. 8 — A plot of echo amplitude as a function of frequency obtained from present spectrometer for Co@C (^{59}Co NMR) (a) 300 K and (b) 77 K.

The results obtained for bulk cobalt and iron confirms specification of our spectrometer matches the performance standard of the spectrometers elsewhere in the world.

7.3 Carbon coated cobalt nanopowder (Co@C)

It is well known from the literature that cobalt phase formation depends largely on method of synthesis, reduction atmosphere and the temperature[26,27]. Zhang *et al.*[28] reported IFNMR studies for the Co@C (average particle size ~20 nm) which are synthesized by the carbon arc discharge method, where they have reported only *fcc* phase. Our sample is synthesised by cobalt carbonyl decomposition or cobalt salt reduction[29-32], having the average particle size of ~50 nm. We have undertaken the IFNMR studies in the Co@C. Spin echo pulse sequence are employed for this measurement with π/2 pulse of 0.5 μs and τ of 15 μs.

Figures 8(a) and 8(b) show the ^{59}Co NMR spectra for Co@C at 300 K and 77 K, respectively. The two peaks observed at 213 MHz and 217.6 MHz, are assigned to the domain walls and domain of the cobalt particles in the *fcc* phase. At 77 K, the peaks get shifted to 216 MHz and 220 MHz due to the increase in the spontaneous magnetization. Additional peaks observed around 212-214 MHz at 77 K are assigned to the grain boundaries of the cobalt, following the interpretation of the Andreev *et al.*[22] It should be noted that the spin echo signal corresponding to the grain boundaries is of higher amplitude at 77 K, compared to that at 300 K. Search for the anticipated NMR signal corresponding to *hcp* phase of cobalt was not successful because of the absence of *hcp* phase. Absence of *hcp* phase in this sample was earlier confirmed from the *XRD* results (section 6). Our observation of single phase of Co@C is in agreement with the IFNMR studies carried out by Zhang *et al.*[28] however they have not commented on the NMR signals arising from the grain boundaries of the Co@C. Our studies have clearly indicated the spin echo signal due to grain boundaries which is additional information about the Co@C. This may

be due to the size of the particle or method of synthesis.

This confirms that our instrument is sensitive enough even to study the nanomaterials. The work is under progress to study the IFNMR in iron oxide nanomaterials, spinel ferrites, hexaferrites, spintronic materials and Heusler alloys.

8 Conclusions

Pulsed IFNMR spectrometer is built and tested in the laboratory and optimized using the standard signals in many NQR samples. Further, ferromagnetic cobalt, iron and Co@C are used as test materials to identify the sensitivity range of the instrument. The results obtained from our spectrometer are in good agreement with the earlier reports. The IFNMR results of Co@C shows the presence of grain boundaries which appears to be first report in this sample. The homemade IFNMR spectrometer is capable of working in the range 10-230 MHz; extendable up to 400 MHz is now available in the country.

References

1 Wurmehl S, Jacobs P, Kohlhepp J T, Swagten H J M, Koopmans B, Maat S Carey M J, & Childress J R, *Appl Phys Lett*, 98 (2011) 10.

2 Wurmehl S & Kohlhepp J T, *J Phys D Appl Phys*, 41(2008) 173.

3 Jordan A, Scholz R, Wust P, Fähling H & Felix R, *J Magn Magn Mater*, 201*(*1999**)** 413.

4 Sukumar U K, Bhushan B, Dubey P, Matai I, Sachdev A & Packirisamy G, *Int Nano Lett*, 3 (2013) 1.

5 Xu Y, Mahmood M, Li Z, Dervishi E, Trigwell S, Zharov V P, Ali N, Saini V, Biris A R, Lupu D & B D Biris, *Nanotechnology*, 19 (2008) 435.

6 Pankhurst Q A, Connolly J J & S K Dobson J, *J Phys D Appl Phys*, 36 (2003**)** 167.

7 Kelgenbaeva Z, Omurzak E, Takebe S, Sulaimankulova S, Abdullaeva Z, Iwamoto C & Mashimo T, *J Nanopart Res*, 16(2014) 2603.

8 Marshall W & Johnson C E, *Le Journal de Physique et Le Radium*, 23 (1962) 733.

9 Freeman A & Watson R , *Phys Rev*, 123 (1962) 2058.

10 Stearns M B, *Phys Rev B*, 4 (1971) 4081.

11 Slichter C P, *Principles of magnetic resonance*, (SpringerVerlag series), 1st Edn, (1990) 3.

12 Levit M H, *Spin dynamics: Basics of nuclear magnetic resonance*, (Wiley Publications) 2nd Edn, (2008) 15.

13 Abragam A, *Principles of Nuclear Magnetism*, (Oxford Publications: London), (1960) 19.

14 Gossard A C & Portis A M , *Phys Rev Lett*, 3(1959) 164.

15 http://spincore.com/products/PulseBlaster/PulseBlaster-Programmable-Pulse-Generator.shtml.

16 Hull A W, *Phys Rev* 17 (1921) 571.

17 Portis A M & Gossard A C, *J Appl Phys*, 205 (1960) 205.

18 Kawakami M & Hihara T, *J Phys Soc Jpn*, 33(6)(1972) 1591.

19 Bromer H & Huber H L, *J Magn Magn Mater*, 8 (1978) 61.

20 Toth L E & Ravitz S F, *J Phys Chem Solids*, 24(1963) 1203.

21 Bastow T J &Trinchi A *Solid State Nucl Magn Reson*, 35 (2009) 25.

22 Andreev A S, Lapina O P & Cherepanova S V, *Appl Magn Reson*, 45 (2014) 1009.

23 Hanna S S, Heberle J, Littlejohn C, Perlow G J, Preston R S &Vincent D H, *Phys Rev Lett*, 4(1960) 177.

24 Robert C & Winter J M, *Comptes Rendus*, 2 (1960) 3831.

25 BudnickJ I, Bruner L J, Blume R J & Boyd E L, *J Appl Phys*, 32 (1961) 3.

26 De La Peña O'Shea, De la Piscina, Homs N, Aromí G & Fierro J L G, *Chem Mater*, 21 (2009) 5637.

27 Dinega D P & Bawendi M G, *Angew* Chem Int Ed, 38 (1999) 1788.

28 Zhang Y D, Budnick J I, Hines W A, Majetich S A & Kirkpatrick E M, *Appl Phys Lett* 76 (2000) 94.

29 Fantini C, Jorio A, Nasibulin A G & Pikhitsa P V, *Material Matters*, 4 (2005) 2.

30 Peng S , University of Science and Technology of China, 2004.

31 Murray C B, Sun S, Doyle H & Betley T A, *MRS Bull*, 15 (2001) 985.

32 Dumestre F, Chaudret B, Amiens C, Respaud M, Fejes P, Renaud P & Zurcher P, *Angew Chem Int Ed*, 42 (2003) 5213.